Semantic interpretation of architectural and archaeological geometries: Point cloud segmentation for HBIM parameterisation

Title

Semantic interpretation of architectural and archaeological geometries: Point cloud segmentation for HBIM parameterisation

Author names and affiliations

Juan Moyano[1]*, Javier León [1], Juan E. Nieto-Julián [1] and Silvana Bruno [3]

[1] Departamento de Expresión Gráfica e Ingeniería en la Edificación, Escuela Técnica Superior de Ingeniería de Edificación, Universidad de Sevilla, 4A Reina Mercedes Avenue, Seville 41012, Spain.

[3] Politécnico de Bari, Department of Civil, Environmental, Land, Building Engineering and Chemistry (DICATECh), Via Edoardo Orabona, 4, 70125 Bari, Italia.

Corresponding author

Juan Moyano. jmoyano@us.es

Present/permanent address and affiliations

[1] Departamento de Expresión Gráfica e Ingeniería en la Edificación, Escuela Técnica Superior de Ingeniería de Edificación, Universidad de Sevilla, 4A Reina Mercedes Avenue, Seville 41012, Spain.

Highlights

- The application of Brodu and Lague's morphological segmentation algorithm called CANUPO to classify the architectural components
- To recognise common morphological features in heritage buildings, so that complex geometries could be identified
- A semantic segmentation method was followed based on open-source software applications such as C2C that are easy to use by operators, academics and BIM researchers, without the need for programming

Abstract (150 words)

The creation of Cultural Heritage (CH) Digital Twins is based on i) the capture of geometric data using digital technologies (laser scanning and photogrammetry); ii) the processing of the raw data to identify, segment and label the objects; and iii) their conversion into BIM objects. Hitherto, the most extensive method for BIM segmentation and modelling is manual, which led to research into the automation of this process, also in the field of CH. Manual operations are still labour-intensive and mathematical approaches are not inclusive for all CH specialists. In this context, this research studies the application of Brodu and Lague's morphological segmentation algorithm called CANUPO to classify the architectural components of the façade of the 16th-century Casa de Pilatos Palace in Seville, Spain, from a Terrestrial Laser Scanning (TLS) point cloud dataset. In this paper, the experimentation on semantic segmentation was

carried out using open-source software, specifically the CANUPO algorithm integrated into CloudCompare software.

Keywords

Historic Building Information Modelling (HBIM), automatic segmentation, laser scanning and photogrammetry, segmentation algorithm CANUPO.

Introduction

In recent times, 3D modelling has received special attention in the Archaeological and Architectural Heritage field. The models must contain precise construction characteristics to be representative of Cultural Heritage (CH) reality. For this purpose, data acquisition techniques that allow Building Information Modelling (hereinafter, BIM) software to build geometries from point clouds are used. Modelling the CH requires completeness and accuracy, which are necessary for comprehensive representation. Therefore, the use of massive data capture techniques such as Structure-from-Motion/Multi-View-Stereo (SfM/MVS) and Terrestrial Laser Scanning (TLS) is increasingly being adapted to a BIM process applied to heritage. This allows Digital Twins to be exported to BIM platforms for parametric modelling. However, the BIM representation is a complicated and resource-intensive process when the built elements belong to CH. The difficulty of modelling existing objects in historic buildings with structural deformations and complex shapes is still a weakness of the HBIM process [1,2] The new BIM paradigm relies on the building information model to improve the efficiency of construction operations, maintenance, and the project life cycle. It also becomes a container to record and catalogue sometimes unexplored information [3].

Nevertheless, the problem lies in the automatic segmentation procedures for subsequent element modelling. This is the case, for example, for complex façades that are common in architectural heritage, whose SfM or TLS range clouds contain hundreds of million points. These files are difficult to handle, even for the manual segmentation of the elements. Two decades ago, when computers were not present in the area of architecture and heritage, the way of segmenting in traditional drawings was to structure the compositional units of a historic building façade according to the hierarchy of its elements. With the emergence of the new BIM paradigm, Murphy et al. [4] were the first to work with parametric models of Renaissance architecture from point clouds using a cross-platform software system. The work was conceived as a simple visualisation tool that structured the elements through a grammar of ornamentation and composition that they called linguistic analogy. The shape grammar can recognise architectural styles and can be divided into a set of basic shapes. This is the procedure currently being carried out in semantic segmentation.

In recent times, researchers and academics are striving to achieve processes that help recognise historical architectural features using learning techniques based on Deep Learning (hereafter DL) [5] at an appropriate level of detail. However, the use of neural networks for point cloud segmentation may limit the operator usability. Even when undertaking segmentation by artificial intelligence, point cloud files contain such a large amount of data that they may not be operational with current hardware and software. It is therefore necessary to develop new strategies related to the interoperability of accurate modelling systems [6], and especially those related to data management.

In this work, an experimental process was developed to demonstrate the applicability of Brodu and Lague's algorithm [7]. This was carried out with a TLS point cloud of a façade of the 16th-

century Casa de Pilatos Palace in Seville, Spain. This algorithm, available as a plug-in called CANUPO in CloudCompare software [8], works as a 3D multiscale classifier by training elementary binary classifiers.

Brodu and Lague developed the system on a natural scene subset to recognise rocks, vegetation, water, and gravel in a riverbed. However, these authors aimed at experimenting with the geometric fidelity that semantic segmentation can achieve to classify architectural elements under the training of this software. These tests have not been applied before; thus, this is an original methodology. The results are compared with manual segmentation to evaluate the selected point set and, once the results of the subsets are obtained, the BIM is created, and the suitability of the data for accurate 3D geometric reconstruction is examined.

Literature review

3D reconstruction is the process by which a computer replicates the physical characteristics of a real object. The shape and appearance of the three-dimensional object or volumetric scene are recovered by analysing the digital information provided by different types of sensors [9]. Therefore, the main objective is to obtain an algorithm capable of representing the connection between the point set from data acquisition techniques and transforming it into a surface shape, be it triangles or any other surface. Applications in the CH field are increasing [10] and becoming particularly challenging when it comes to establishing the maximum fidelity in the 3D reconstruction [11]. Most studies on parametric element reconstruction from range clouds focus on the representation of planar surfaces [12], independent elements with no information about their relationships. This means that there is also no relationship between the elements and their morphology. In this way, to establish a connection between an element and its function, the first step is to analyse the object shapes and to perform semantic modelling of the compositional elements (classification of their shapes). An example of semantic modelling is the work by Gaiani [13] on the Altar of the marble shrine of Augustus. This analysis determines the simplification degree when the objects are not separate but form an architectural ensemble. Previous studies addressed the classification of building components. This classification usually appears as identity coding of architectural elements in architectural treatises [14] and could be related to the hierarchical description of building components.

The scientific literature has attempted to analyse the geometric quality of the 3D model [15] by evaluating its accuracy based on the LiDAR survey. Here, the level of detail of the model depends on the point cloud resolution. However, current digital BIM platforms cannot handle records with an excessive amount of information in the range clouds. Therefore, it is necessary to establish the procedures involved in the transformation of these point sets into a Heritage BIM project (HBIM) and, secondly, to know how these processes can be optimised. When approaching the modelling of a restoration project, the identification of the geometric characterisation (architectural morphology) can be articulated around two points of view [14], the raw processing of the dataset in the digital model and the use of the semantic information produced by the design model. The former refers to data acquisition processing in the form of Massive Data Capture Systems (MDCSs), and the latter is supported by a BIM tool; this methodology aims at creating a digital information system associated with graphic documentation [16].

To solve the transformation of the point cloud into BIM parametric objects, several authors have reviewed the extensive scientific literature on SfM data [17–21] and TLS point clouds

[15,22–25]. In this sense, the importance of fields of knowledge such as geomatics and 3D model reconstruction is highlighted. From these efforts to achieve automation of point cloud to BIM processes, the relatively new term semantic segmentation has emerged. According to Yang et al. [26], this is a critical issue. The proposed solution is to limit point sets in subset units whose information can be handled by digital platforms. Thus, Spina et al. [27] used the term point cloud segmentation as a way to process and organise the point cloud into meaningful subsets. This organisation makes it possible to reduce the shape complexity of the raw point cloud and to facilitate the processing of 3D object surveys. The reason the semantic segmentation is useful is twofold: i) point clouds contain information about the actual geometry of the object, but lack semantic information on the categories of objects or materials constituting the building components [28]; ii) point cloud simplification allows to operate in BIM platforms to implement object geometries. Achieving 3D models requires tasks such as segmentation which, according to Aitelkadi et al. [29], is the key step during the point cloud processing to identify homogeneous areas. Thus, most of the segmentation focuses on the information from the point cloud.

The extraction of semantic features was summarised by Pu et al. [30], who determined the optimal values of the segmentation parameters as size, position, orientation, topology, and point density. The proposed segmentation is based on point colour, laser intensity, and geometric data. These strategies involve an automatic identification process without the need for operator intervention. Boochs et al. [31] defined segmentation as the combination of algorithms that improve projective reconstruction. Grilli et al. [29] defined it as the process of grouping "point clouds into multiple homogeneous regions with similar properties, while classification is the step that labels these regions". Classification as outlined by Grilli et al [29] is based on the need to bring the point cloud into the BIM software through identification. In other words, the aim is to determine the meaning of function and shape in the 3D elements, although most segmentation algorithms work with a 2.5D surface model hypothesis [32].

Supervised methods require a preceding training phase for the classification solution. Previous studies focus on identifying vertical elements such as walls, floors, or those limited by floors [33] or other elements. They can also integrate the knowledge of specific elements into the point cloud, especially to develop interior elements [28,34,35]. Grilli et al. [29] reviewed and classified segmentation algorithms as those based on edges [36] and data [37], region growing segmentation [38], or model fitting segmentation based on point fitting using RANSAC programming [27,39]. An approach based on decomposing architectural structures into geometric primitives (planes, cylinders and spheres) might seem suitable for their mathematical adjustment via parametric object modelling (BIM) algorithms. However, the use of these algorithms is sometimes not within the reach of regular BIM operators. The reason for this lies in the software usability, which requires mathematical processes; secondly, because not all point cloud files are valid since they may or may not be structured. Most segmentation algorithms work with structured or LiDAR files.

Generation of geometric construction models

Newly constructed buildings respond to a project theory based on volumes, new materials and forms of construction. On the contrary, the built CH (historic buildings) is the result of numerous transformations over time and is subject to building components constructed at various periods depending on the refurbishment carried out.

The generation of parametric as-built 3D models from massive data acquisition is a reality for complex surfaces of historic buildings. Over time, several attempts have been made at semi-automatic methods that allow the creation of parametric models from point clouds [40], focusing on model accuracy [41]. Other approaches use curves and NURBS surfaces to reconstruct complex objects [42] without oversimplification. The advantage of creating parametric objects on digital BIM platforms is that the resulting products are dynamic objects that can be transformed instantaneously [43]. However, this process is ideal for reconstructions where the objects are ideal models from architectural manuals or libraries within specific software. The complexity of historic architecture goes beyond this. Therefore, parametric 3D reconstruction from digital twins captured by TLS or SfM is a knowledge gap. The aim is that both architectural and archaeological elements modelled on digital platforms should represent the greatest geometric similarity to real objects, essentially to preserve their characteristic geometric uniqueness.

The model associated with the structure ensemble offers the opportunity to relate the accuracy of the HBIM to the level of detail (LOD) needed. To do this, some researchers [44] used various workflows based on mathematical algorithms, such as software applications including Rhino-Grasshopper [40] and Dynamo [45], which interact with programmes such as Graphisoft ArchiCAD or Autodesk Revit. Thus, 3D reconstruction models with complex architectural shapes are automatically generated as well as through NURBS surfaces. Yet, the use of several software packages limits the work of BIM operators. The true nature of accurate 3D reconstruction is to automate processes by reducing the number of software applications used. This is the knowledge gap of 3D Accuracy Reconstruction Geometry (3D ARG).

Semantic segmentation

Reverse engineering is the process of capturing massive data from LiDAR technology. Therefore, it is an accurate representation of the building shell and its superficial elements. These data are recorded in files with a large amount of information that are not operational on a BIM platform. The 3D point cloud shapes fundamental parameters capable of representing both geometrical components and radiometric elements [29]. Due to the large amount of information they provide, there are numerous research studies on the subject. One important area is segmentation algorithms for automatic classification [5,27,28,36,46,47]. Recently, a large-scale open platform for point cloud processing has emerged. The Point Cloud Library (PCL) framework contains numerous state-of-the-art algorithms for filtering, surface reconstruction, model fitting, registration, and segmentation, among others [48]. A review of these algorithms was carried out by Grilli et al. Hence, for this research, those for model fitting are the most interesting algorithms. In the field of image analysis and processing, the concept of semantic segmentation aims to classify each pixel of a scene image. Each pixel is then allocated to a group in an image, resulting in homogeneous clusters [49]. The most widespread use of this technique is in the fields of autonomous vehicles, robotics, and indoor positioning systems [5]. This classification is possible thanks to automatic processes based on Machine Learning (ML). This technology applies inferences to a given piece of information to appropriately represent relevant aspects. Thus, segmentation studies are crucial for planning sustainability strategies and on perception criteria [50]. Segmentation uses ML or Deep Learning (DL) techniques; their difference lies in the types of algorithms they implement. ML uses mathematical algorithms, whereas DL is based on biological neural networks of the human brain [51]. Segmentation within the digital documentation of CH uses these learning techniques to identify objects. The novelty is the combination of these techniques to work

with point clouds. Here, the method represents considerable benefits in shape detection for further modelling in heritage environments. The feature classification can be conducted via pre-training, but also through pre-set training and the interactive method, where complex mathematical procedures [29] are required to achieve appropriate results. Even so, the use of these technologies in the three-dimensional domain is rather limited. Some studies used these methodologies on historical facades to apply 2D to 3D information transfer [52], while other methods performed semantic point cloud segmentation [5]. These can be conducted by creating a set of images through the point cloud (Multi-view based), point cloud rasterisation based on voxels, or by applying a feature-based approach to the points.

Other methods related to the above exist in the scientific literature. There are methodologies involving training from an original (zero) position with previous training of readjustment or hyperparameter optimisation (impulse, weight drop, or learning rate) [51]. On the other hand, there are some studies on artificial neural networks (ANN) that can recognise objects, such as 3D ShapeNets [53], or PointNet [54]. Other studies focus on obtaining vector values from photographs. The classification is performed through three parameters using freely available software such as AutoTrace, Potrace, or Inkscape. The process consists of interpreting a bitmap in black and white to produce vectorised curves [55]. For an in-depth analysis of a polygonal model, other studies simplify complex 3D geometry into a series of 2D closed polygons by automatically converting each polygonal section into a raster model. All raster sections produce a 3D volumetric model in a voxel format. This process is called voxelisation [56][57]. Here, the voxel is to 3D what the pixel is to 2D, i.e. the voxel is the minimum unit to form a volume. A series of voxels, endowed with information such as position, colour, and density, allow the generation of a hypothetical 3D model [58]. This methodology intends to reduce the file size, thus reducing the work time as the computations would be much faster [59]. In addition to its use in visualisation tests such as x-ray imaging or MRIs, this method is also used to detect 3D objects in robotics and autonomous driving [60]. Given that this approach is used when high accuracy is required, it could be beneficial for virtual heritage recovery. One of the most interesting options for CH modelling could be working with point clouds directly without creating meshes. In this sense, it is proposed to use this methodology to automatically convert the point cloud into parametric objects, although it would still be necessary for the user to operate the programme [57].

Methodology

1.- Case study

The façade of the Casa de Pilatos, a 16th-century Palace located in the centre of Seville (Spain), was chosen as a case study for semantic segmentation. The façade composition is based on planes and decorative elements of different architectural styles and with different shapes. Thus, the case study is a suitable environment for 3D point cloud data segmentation.

2.- Data acquisition

Image-based methods and 3D laser scanning are the most widely used professional and scientific data acquisition techniques for large-scale projects. Of these two techniques, TLS is currently the most extensively used, as it provides accuracy and speed. Notwithstanding, other researchers have used image-based methods for 3D reconstruction because of their economic advantages, efficiency [61], and to ensure fidelity in CH BIM [21,62]. LiDAR technology is based on the calculation of the distance between the laser and the object. This procedure is developed using the time-of-flight method or through the transmitted and received signal

267 waveform [18]. The method performs a scan of the entire surface to capture thousands of
268 points in an x, y, z coordinate system to produce the range cloud. In this case study, a Leica
269 Geosystems BLK360 laser scanner is used to capture the geometry of the main façade of the
270 Palace. This device uses the Waveform Digitising (WFD) technology and has four built-in
271 cameras: 3 digital HDR, colour sensor and fixed focal length cameras (2592 x 1944 pixels
272 resolution, 60° x 45° (V x H), a full dome of 30 images, automatic spatial rectification, 150 Mpx,
273 360° x 300°); and an infrared camera (160 x 120 pixels resolution, 71° x 56° (V x H), a full dome
274 of 10 images, 360° x 70°). Although the equipment can be controlled using a computer or a
275 tablet, the data capture was automatically performed and further processed in the laboratory.
276 Additional specifications of the scanner are shown in Table 1.

LEICA BLK 360			
Wavelength		830 nm	
Field of view	360º (horizontal)/ 300º (vertical)		
Range	Min. 0,6-up to 60 m		
Point measurement rate	Up to 360000 pts/sec		
Ranging accuracy	4mm @ 10 m/7 m @ 20m		
3D point accuracy	6mm @ 10 m/8 m @ 20m		

277

278 Figure 1 depicts the research workflow:

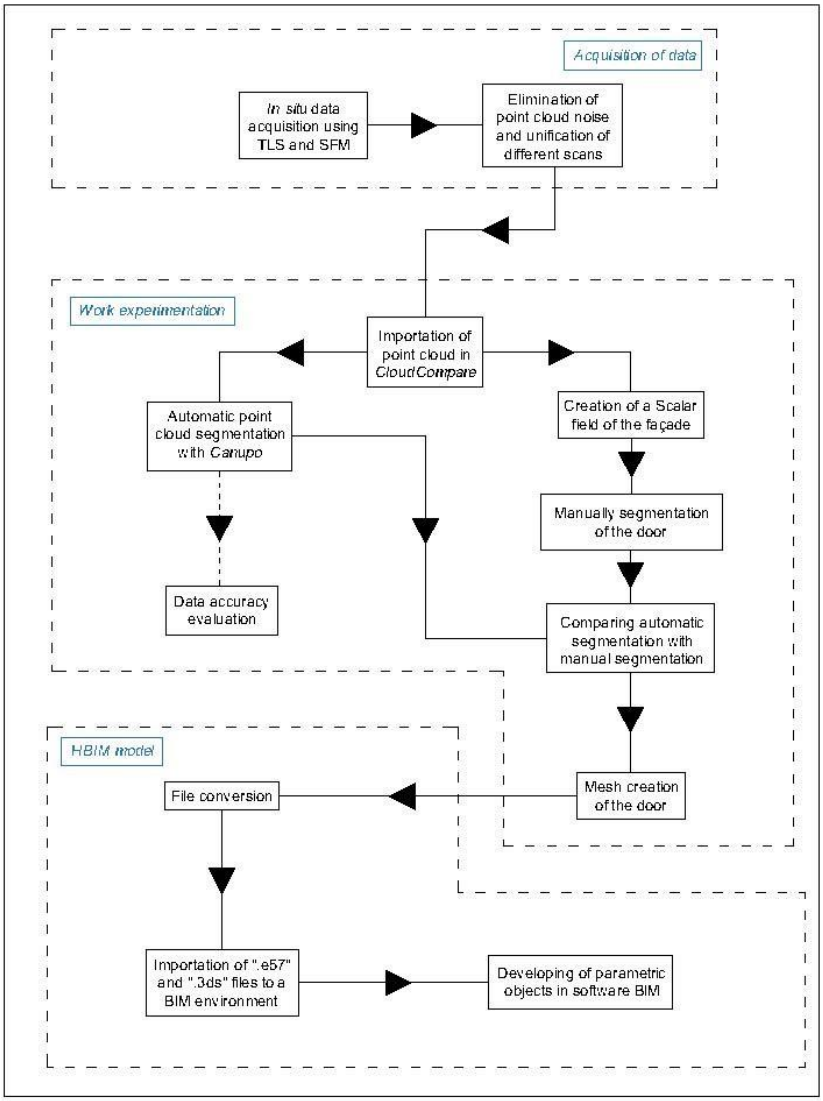

Figure 1. Workflow.

3.- Post-processing

Point cloud processing involves interpreting the spatial components (x,y,z). The segmentation and classification of the object are necessary for 3D modelling and the analysis process in the research into historic buildings. To prepare the dataset, a filtering of the elements outside the range of the main façade is carried out on the TLS global cloud. Points containing residual values and outliers are removed using the Leica Cyclone 9.2.1 software (Leica Geosystems, 2018). In the segmentation process, the homogeneity criterion is not related to the image radiometry. The classification of the morphology structure component will be the selection criterion. Therefore, the façade surface is partially taken, considering its composition based on planes and decorative components. The point cloud, with 38 million points, is obtained and transferred to CloudCompare v2.10.2 (Zephyrus) software (Girardeau-Montaut, 2003) for further processing. From the C2C process, two point subsets are obtained from the façade: a manually segmented group of elements and the global range cloud. In the 3D point cloud classification, three types of discrepancies must be taken into account, such as i) the gaps in the cloud due to laser beam occlusions, ii) the effects that may be caused by shadows on the scanned elements, and iii) those figures in movement through the architectural spaces.

4.- Evaluation of the experimental design

The 3D object reconstruction is an important step in digital representation since it allows for approaching the physical world as a basis for analysis and construction [31]. These objects in historic buildings generally have complex geometric elements, as in the case of natural shapes such as trees, rocks, and grass. This paper hypothesises that Brodu and Lague's algorithm [7], which was developed for these complex terrain geometries, should apply to the morphology of heritage buildings. Also, to the best of our knowledge, this algorithm has not been applied to heritage elements before. This algorithm is effective in the classification of natural surfaces through the local analysis of changes in the geometrical properties of the point cloud. It is available in CloudCompare software [8] as the CAracté-risation de NUages de POints (CANUPO) plug-in to work as a 3D multiscale classifier by training elementary binary classifiers. The basic working principle of this algorithm is to project a sphere with a radius depending on the working scale onto a point in the scene; next, the geometrical behaviour of neighbouring points in three dimensions is analysed in this space. Brodu and Lague applied this system to natural scenes of a subset with a range of scales to recognise rocks, vegetation, water, and gravel in the Otira riverbed (New Zealand). The procedure relies on the combination of C2C classifiers, working in two different ways. The first approach executes the "Classify" command, using the available classifiers created by default. The second method creates customised "Train Classifier" classifiers. Once the point cloud is obtained, the system performs training through different parameters: the measurement range, measurement scale, and point sampling. Yet, the idea behind the classification procedure is the combination of scales, where dimensionality makes it possible to distinguish from more than one category [7]. The mathematical rationale was made explicit in section 3.1 Local dimensionality at a given scale.

4.1.- Manual segmentation through the scalar field

The evaluation process is carried out by means of a complementary study and analysis. To this end, a point set from manual semantic segmentation comprising three testbeds is obtained. This process is common in scientific literature. Kovanič et al. [63] used manual segmentation to process point cloud data and determine the geometric parameters of a rotary kiln. Li et al. [64]

used manual segmentation to automate the analysis of building facades from TLS. The purpose was to semantically segment and label the depth planes. Manual refinements are sometimes used in point cloud segmentation in tree structure studies [65]. However, manual segmentation involves a laborious and time-consuming task. The more complex the scene is, the more difficult it is to process [66]. The main challenge is to match the morphology of the architectural elements. Likewise, because it is a manual process, the point subsets taken may or may not belong to the geometry of the chosen element. Considering the limitations of manual segmentation, a scalar field is created to classify the façade's point cloud according to values on the "y" axis, as established by the C2C software's coordinate system (Figure 2).

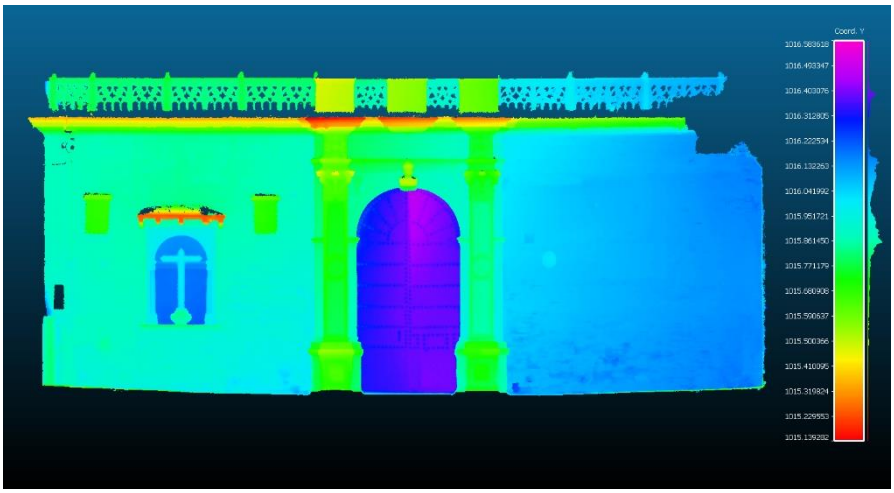

Figure 2. Façade's scalar field.

This process involves classifying the points in space with respect to a (x,z) plane. In other words, the distances from the point cloud to a theoretical (x,z) plane are being calculated. The result of the process is a scalar value for each point in the cloud that indicates the Euclidean distance between the analysed point and the closest point to the imaginary plane. The results are displayed in the histogram in Figure 3.

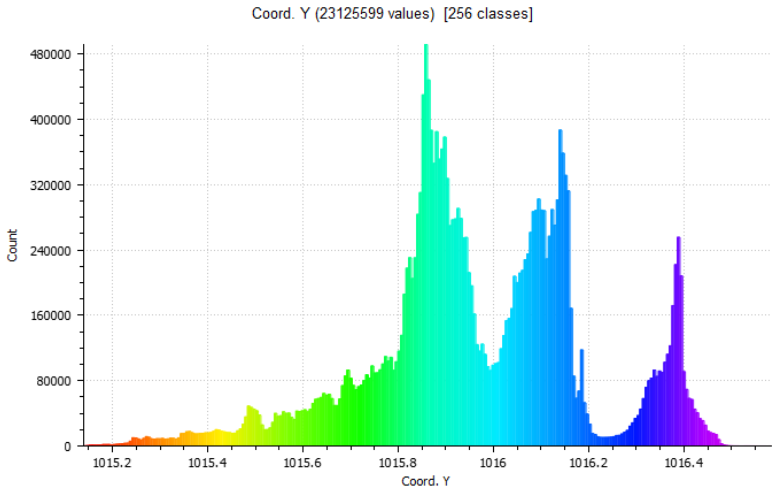

Figure 3. Histogram of the number of points between the reference plane (x,z) and the Y-coordinate.

It should be noted that manual segmentation may capture points outside the chosen model since there would not be a segmentation of classification with certain parameters.

4.2.- Algorithm validation testbeds

In order to test the applicability of the classification algorithm, three testbeds were carried out. First, working with the global point set, i.e. considering the complete façade (21.00 metres long by 8.50 metres high (Figure 4)), the parameters were adjusted according to the length of each element.

Marble shapes were initially differentiated from the predominant brickwork: the three parameters involved in the process were minimum distance, interval, and maximum distance. The minimum distance is the smallest magnitude between the elements to differentiate. For example, the length of a brick or a rivet in wooden doors, among others. The maximum distance is the opposite, the largest dimension of the elements. In this case, the height of the pilasters that form the centre of the marble doorway was considered. Finally, the intervals to determine the total number of scales needed were chosen.

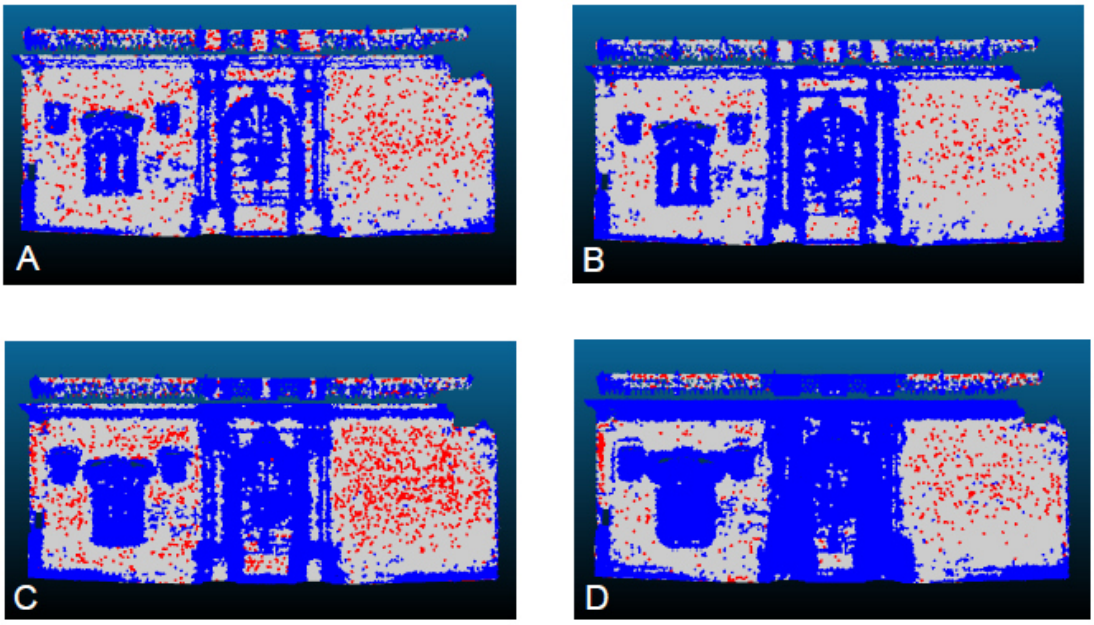

Figure 4. (**a**) Test A; (**b**) Test B. Classification through the CANUPO plug-in. The red dots represent the bricks and the blue dots represent other materials.

The images show the point density of a scene represented in the proposed feature space at different scales. Each image represents the working process with the C2C tool to measure the distances for the chosen architectural elements. Meanwhile, the larger the maximum distance, the longer the processing time. Similarly, the smaller the interval, the longer the processing time. In the analysis, tests were conducted by choosing alternative measurements according to Table 2.

Table 2. Distance parameters taken for global façade processing

	Min. Distance (m)	Step (m)	Max. Distance (m)
Survey A	0.01	0.025	0.50
Survey B	0.01	0.01	0.50
Survey C	0.01	0.01	1.00
Survey D	0.01	0.01	1.50

Also, various graphs were produced to evaluate the data obtained and to verify the software performance. Comparisons were carried out of the tests in which the processing time, the number of classified points, and the precision of each sample of the sets were represented. It should be noted that the processing time depended on the hardware used, a computer of average specifications (Intel i5 processor with 12 GB RAM). Each step was measured (Figure 5). The number of classified points represents the subsets that can later be used to generate meshes for conversion into parametric BIM objects. The accuracy is a magnitude achieved through the experimental values entered into the software. For example, for this case, measurement distances of 10 cm were taken.

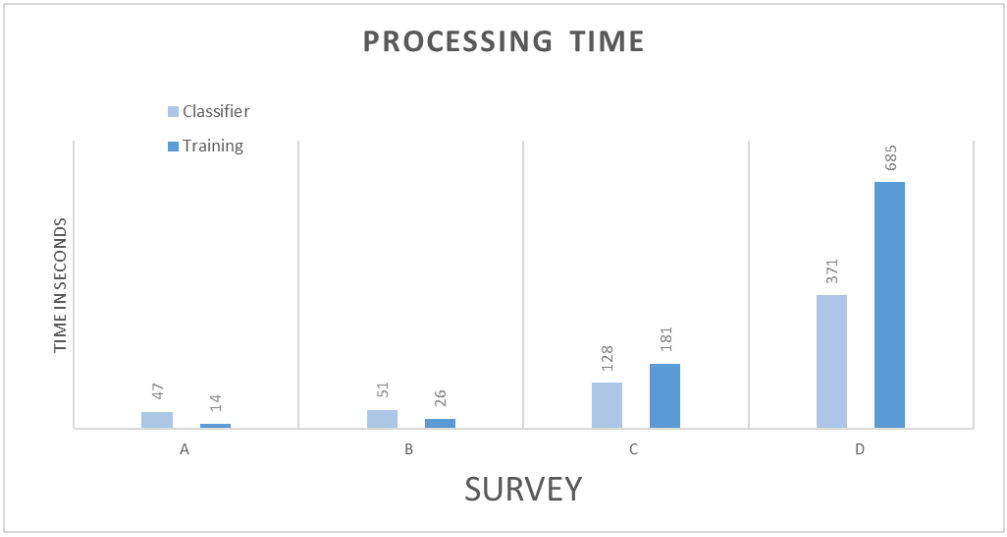

Figure 5. Processing time for each test A, B, C, and D of the training and classification using the CANUPO algorithm.

Following the classification procedure, the best combination of selection scales was defined. The operator can then determine the scale range of the different categories and elements to be geometrically classified. According to Brodu and Lague, the algorithm finds the best combination of scales to segment into different categories previously defined by the operator, as shown in Figure 6.

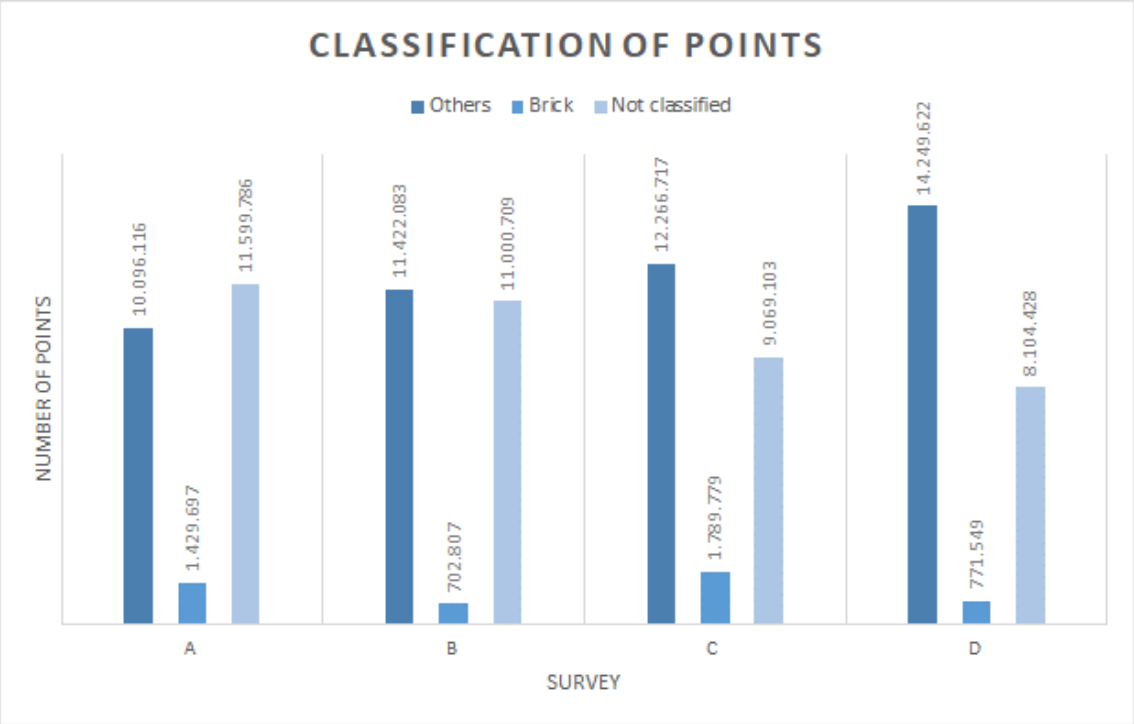

Figure 6. Point classification in the global façade. Tests A, B, C, and D.

Figure 7 shows the Balanced Accuracy (BAa) value. With this value and that of the FDRfdr (Fisher Discriminant Ratio), the performance can be measured by classifying each point in its respective class. This data appears as a supplement in the statistics section once the first phase, the training, is carried out. The result of this phase is a .prm file.

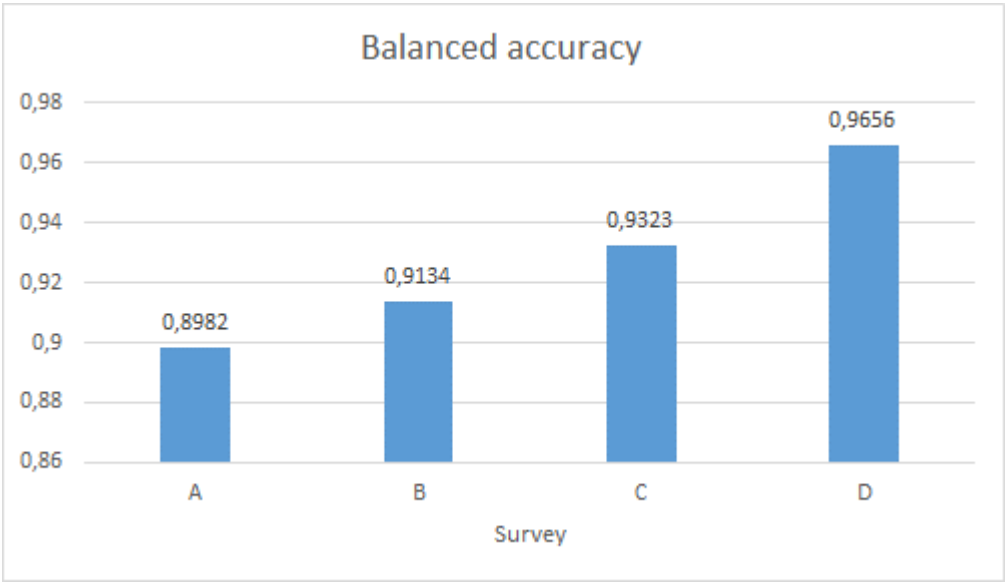

Figure 7. The accuracy achieved in tests A, B, C, and D. Sampling over 10,000 points of survey items.

Each test was analysed to determine the classification percentage of points in the façade global point cloud. 49.84% was obtained for survey A, 52.43% for survey B, 60.78% for survey C, and 64.95% was achieved for survey D.

Figure 8. The schemes of the three testbeds.

The second testbed addresses the main entrance to the Palace, focusing on the area delimited by the two pilasters and the lintel of the portico (3.50 metres wide by 7.55 metres high). The hardwood door is selected, the marble pilasters are differentiated, and the brickwork is omitted (Figure 9).

(a) (b)

405 **Figure 9.** (**a**) Test E; (**b**) Test F. Classification through the CANUPO plug-in.

406

407 **Table 3.** Distances taken to process the façade portico.

408

	Min. Distance (m)	Step (m)	Max. Distance (m)
Survey E	0.01	0.025	0.50
Survey F	0.01	0.01	1.50

409

410 The same procedure enabled comparisons of the tests by plotting the accuracy obtained, the
411 processing time, and the number of classified points for each data set sample.

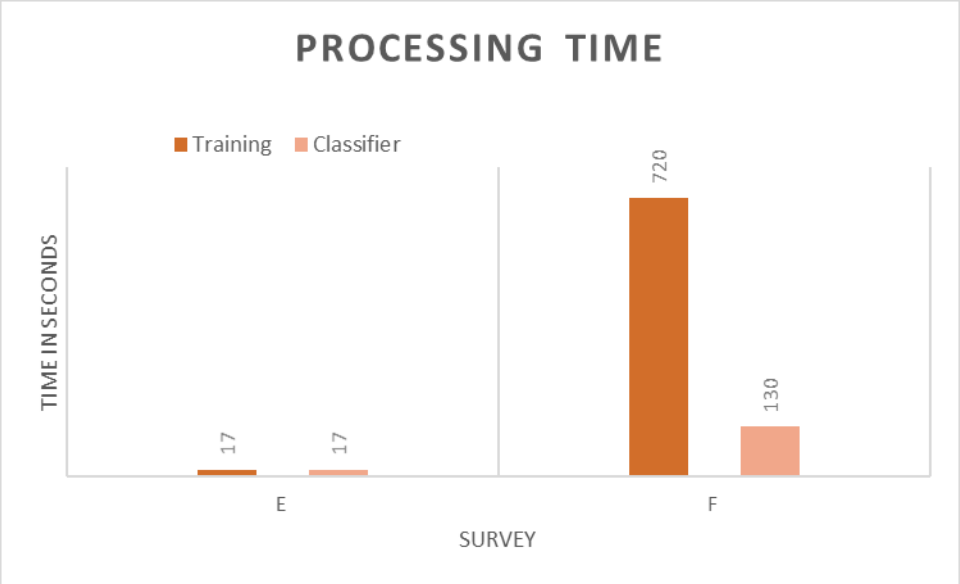

412

Figure 10. Processing time for the training and classification tests E and F using the CANUPO algorithm.

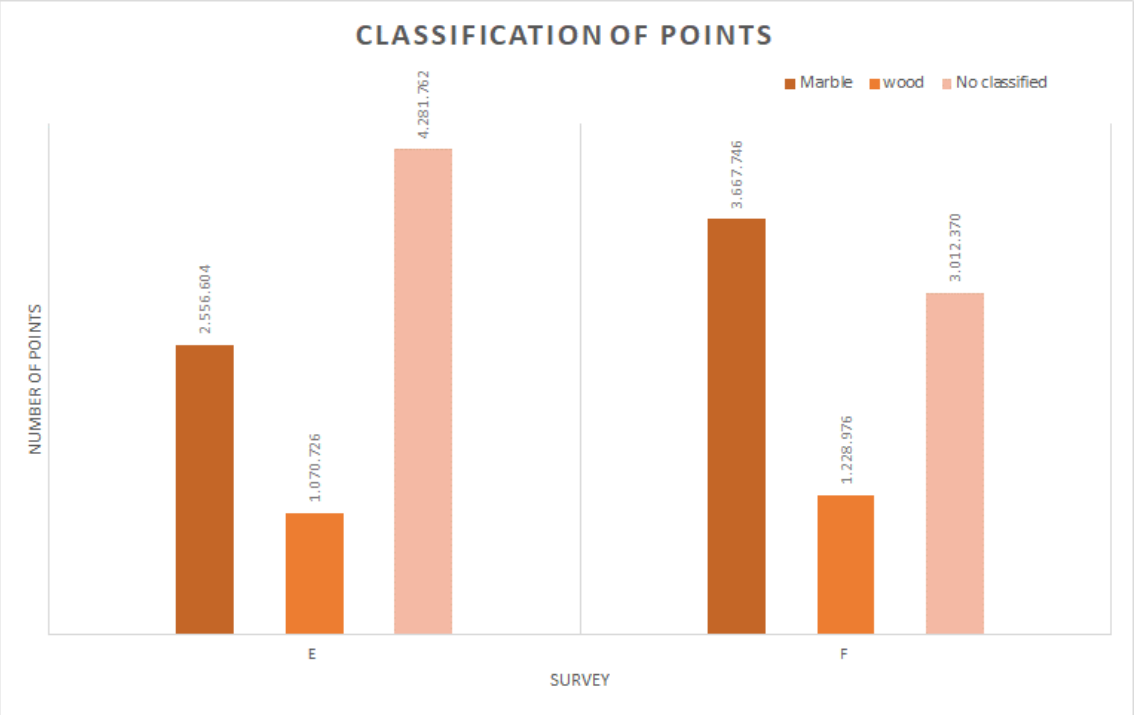

Figure 11. Point classification of the façade portico in tests E and F.

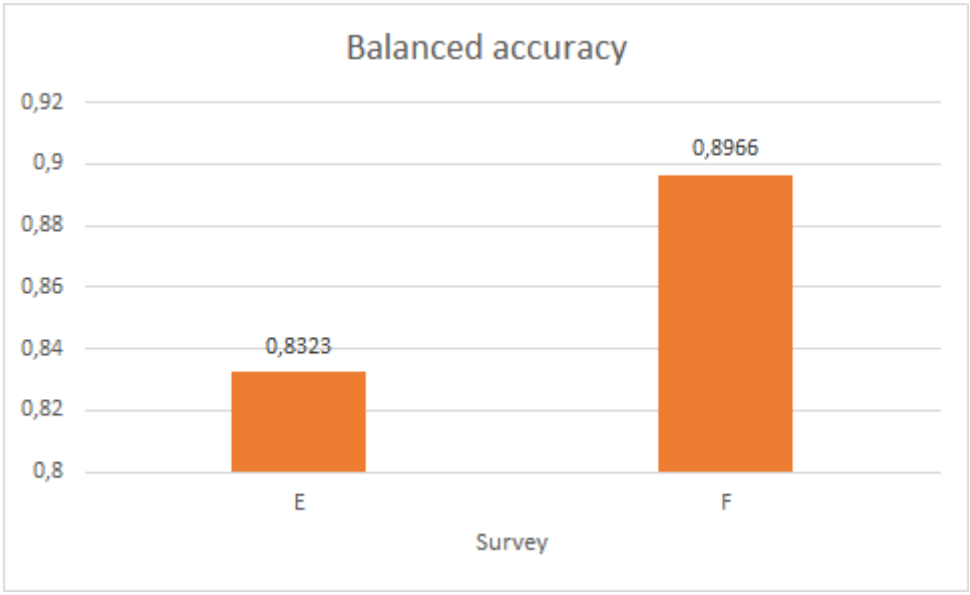

Figure 12. The accuracy achieved in tests E and F of the marble portico and the wooden door. Sampling over 10,000 points of study elements.

Regarding the percentages of points classified in the façade portico corresponding to the two materials analysed, the marble of the entrance portico and the wooden door, 45.86% was obtained in survey E and 61.91% in survey F.

For the third testbed, the retable on the left side of the façade was chosen. It is a piece carved in different marbles in various shades of colour. The dimensions of the chosen area are 1.75 metres wide by 2.35 metres high, as in the marble frame. It has been chosen for its morphological singularity, a miniature retable composed of two columns on a round arch and a Christian cross in the centre (Figure 13).

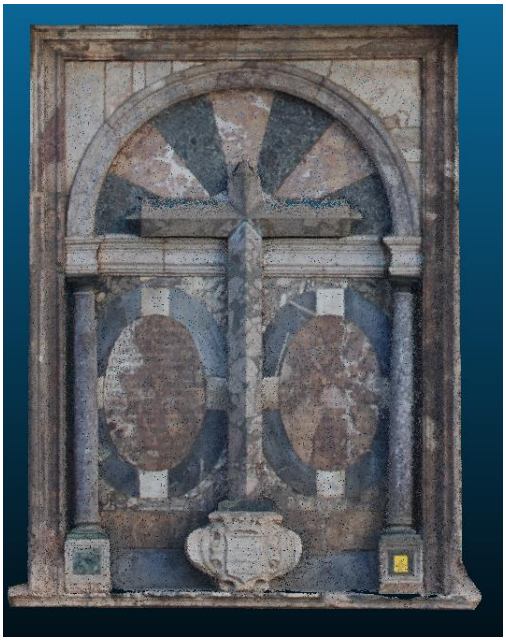

Figure 13. Processing time for training and classification tests E and F using the CANUPO algorithm.

Figure 14. (**a**) Test G; (**b**) Test H. Classification through the CANUPO plug-in.

The results of tests G and H are shown in graphs according to the accuracy achieved, the processing time, and the number of classified points of each data set sample. The distances taken for the processing of the retable are shown in Table 4.

Table 4. Distances taken to process the retable.

	Min. Distance (m)	Step (m)	Max. Distance (m)
Survey G	0.01	0.025	0.50
Survey H	0.01	0.01	1.50

Next, comparative tests were carried out, and the processing time is shown in Figure 15.

Figure 15. Processing time for training and classification tests E and F through the CANUPO algorithm.

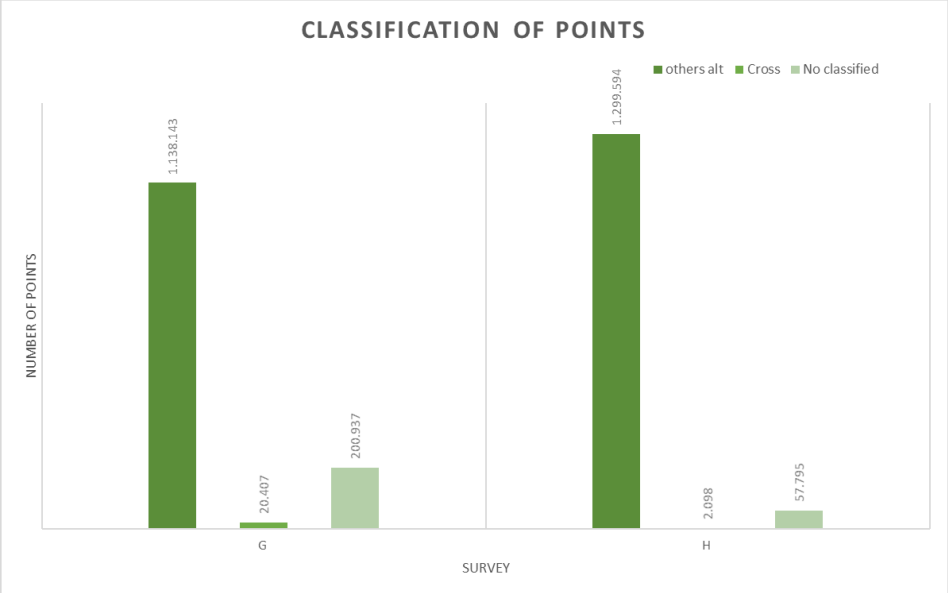

Figure 16. Point classification on the façade portico in Tests G and H.

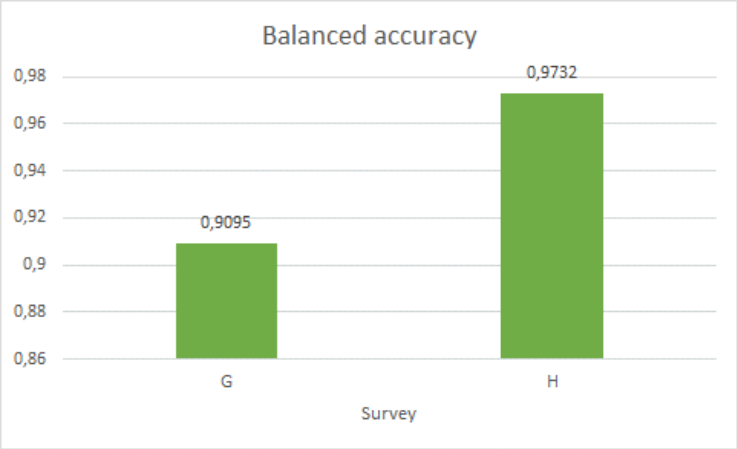

Figure 17. The accuracy achieved in tests G and H. Sampling over 10,000 points of survey items

The point classification percentage in the retable (different types of marble in various colours) was also determined. 85.22% was achieved in test G, and 95.75% in test H.

CloudCompare software using the CANUPO algorithm allows the operator to obtain a probabilistic classifier. This classifier firstly defines the projection of the data onto a plane of maximum separability to, secondly, separate the classes. The main advantage of this is that an immediate and intuitive visualisation of the classification process (Figure 18) is obtained. The reliability level is set on the abscissa axis and the ordinate axis sets the range.

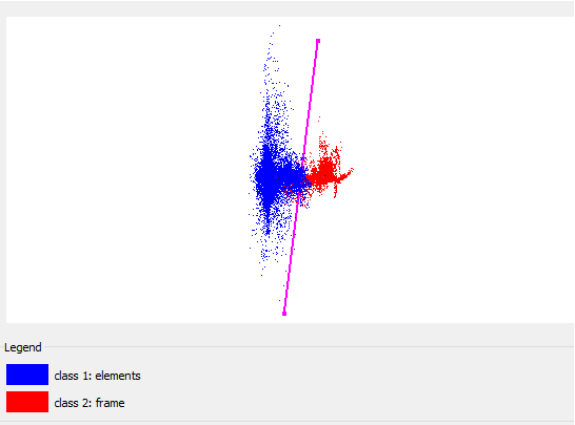

Figure 18. Classifier definition in the plane of separability.

Once the manual segmentation through the scalar field and the point classification process with the CANUPO algorithm have been carried out, the modelling of the gate was undertaken (tests E and F). The gate was segmented according to Figure 19. For the manual semantic segmentation of the point set and its segmentation using the CANUPO algorithm, a reference was established in percentages of the number of points captured; next, the creation of the BIM took place. In this case, the manual segmentation was taken as a reference, with which

2,535 points were obtained. Figure 19a shows (red colour) the projection of the point set selected by the algorithm in tests E and F compared to the total number of manually segmented points of the gate.

(a) (b) (c)

Figure 19. (a) Manually segmented point set, (b) test E, and (c) test F.

The point set taken as a reference was considered 100% of the points (Figure 19 a). 37.27% of the manually segmented points were classified in test E, and 46.71% in test F. Figure 20 shows the number of points of each test.

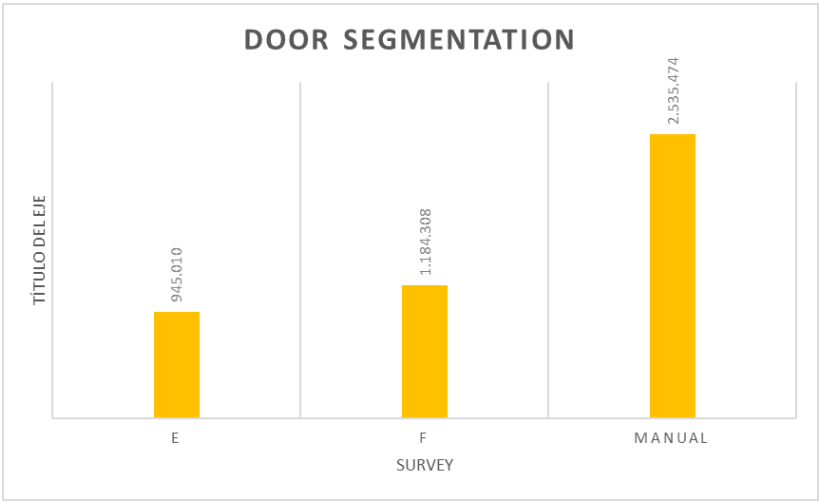

Figure 20. The number of points obtained from segmentation tests E and F against manual segmentation (M).

5.- Modelling the tests in BIM

An important factor in the parameterisation process is determining the geometry. The process of transferring TLS or SfM to BIM is known as Scan-to-BIM [67]. The Scan-to-BIM framework is specifically designed to ensure that BIM meets the applicability requirements for CH, whether architectural or archaeological, by efficiently managing the information provided by data capture techniques. Wang et al. [68] determined four fundamental steps in the process,

including the identification of information requirements, scan data quality, data acquisition, and BIM reconstruction. This involves creating the BIM with the geometric parameters provided by the MDCSs. In practice, the MDCS files are imported into the BIM tools and serve as a reference template for modelling. Nevertheless, this procedure can be prone to errors. To overcome these issues, previous research has addressed the semi-automatic generation of parametric objects from TLS or SfM point clouds. Antón et al [41] evaluated the accuracy of the 3D meshing from remote sensing products to later propose a semi-automatic three-stage procedure to create an as-built HBIM. For their part, Andriasyan et al [40] explored the combination of Rhino+Grasshopper-ArchiCAD combination to automate the Scan-to-BIM process. In this paper, effective procedures to automatically build parametric objects are explored, which is a knowledge gap in the field. To validate the data obtained (the points segmented using the CANUPO plug-in), the workflow by Moyano et al. [69] for complex surfaces common in architecture and archaeology is used.

Surveys M (Manual), E, and F were exported to Rhinoceros in .ASCII or .e57 formats for their conversion into meshes, in the same way as the subset obtained by segmentation through the scalar field. The meshes were inserted into the BIM software (ArchiCAD) to be transformed into .gsm parametric objects, in such a way that the actual geometry of the wooden door was generated. However, the meshes can also be subsequently transformed into 'Morph' elements for editing and customisation in the HBIM project. In this case, the Boolean operations between elements was the procedure chosen. To define the surface faces of the door with a thickness of 8 centimetres, division surfaces were used, thus performing a subtraction with extrusion upwards as an operation between solid elements in the BIM platform. This procedure was carried out for both faces to achieve a model as shown in Figure 21. The model used the manually segmented TLS point cloud, as it was the most complete of all surveys. This procedure verified the Scan-to-BIM methodology for the system requirements. Hence, the parametric modelling was validated for the case of the manually segmented point set from the scalar field of the main façade.

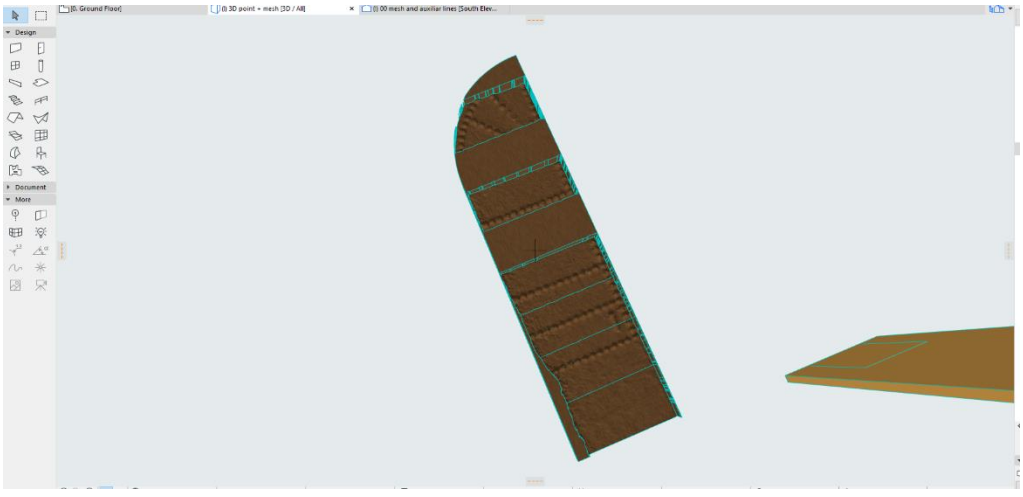

Figure 21. Relief of the wooden door solid object.

5.1 Modelling results

3D modelling has been particularly conducted for civil engineering applications and games based on real-world environments [70]. With a view to approximate real shapes, BIM

technology has implemented processes to manually and automatically create geometric models from point cloud data. The point cloud representing complex architectural shapes can be translated into triangulated meshes before generating the parametric objects. This is a common workflow established by specialists in the field, a further stage involved in the Scan-to-BIM to the Mesh-to-BIM process. That transformation requires using different programmes. Yang et al. [71] followed a three-step process: the extraction of basic primitives in 3D in Rhinoceros software, the transformation of surfaces to volumetric components using extrusion and NURBS functions in the same programme, and the generation of Dynamo visual programming algorithm packages. This process is rather complex and would require that the BIM operators specialise in various software. In this paper, the whole process was carried out using Rhinoceros and ArchiCAD. The result of the tests is shown in Figure 22.

Figure 22. Global point cloud of the façade and BIM of the door.

5.2.- Point cloud decimation validation within the Mesh-to-BIM process

To validate the expected point density of a parametric model, the point set of the manually segmented wooden door was decimated. The data were next taken to the C2C software to reach the desired resolution. Optimal values of the segmentation parameters were also sought so that the smallest number of points would provide representative data for the Mesh-to-BIM process. Test work was carried out starting from 100 points per square metre to know the scope of the work. This point density was initially established by Pu and Vosselman [30] for their experimental work on an automatic method for the reconstruction of building façades. In this paper, the data consist of a point subset of 2,535 points. Using the subsample command with random parameters, a decimated subset of 2,000 points was obtained, which entailed approximately 110 points per square metre (Figure 21). In the second phase, further decimation of 10,000 points spread over the entire surface of the wooden door was carried out, resulting in approximately 600 points per square metre (Figure 22). Afterwards, the Mesh-to-BIM process was performed using Surface Poisson Reconstruction [72].

As a result, through a scalar function adjustment, a bubble was obtained by connecting all the related points. By reducing the density in the SF display parameters, part of the bubble was

removed. The decimation results are shown in Figures 22 and 23, and the histograms of the achieved point densities are presented in Figure 24.

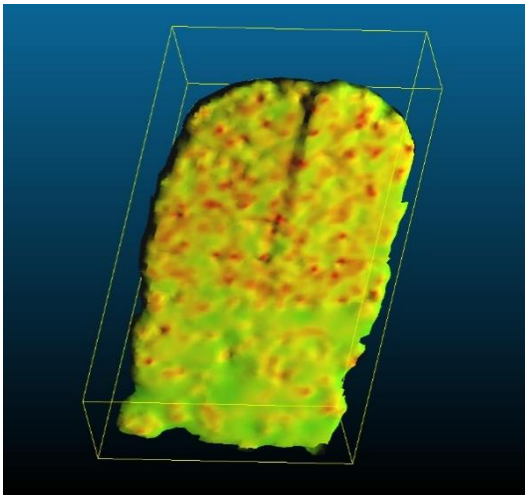

Figure 22. Mesh reconstruction of the survey M point set at 110 points/m2 density.

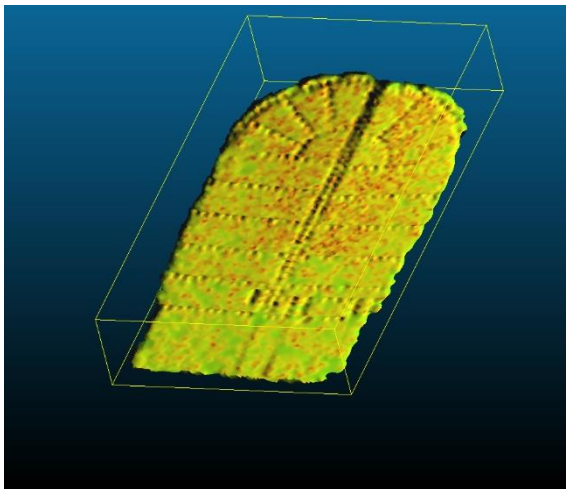

Figure 23. Mesh reconstruction of the survey M point set at 600 points/m2 density.

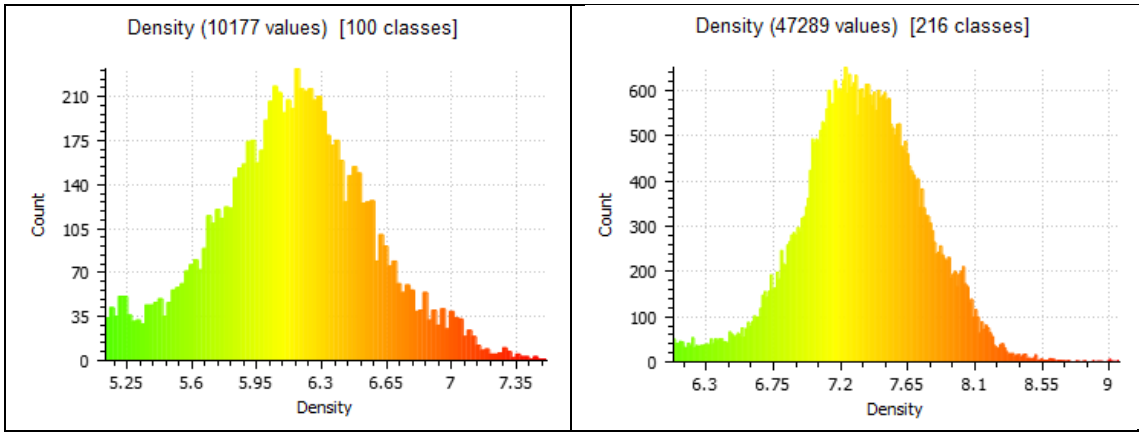

Figure 24 a) Histogram of the survey M point set at 110 points/m2 density. b) Histogram of the survey M point set at 600 points/m2 density.

Discussion of results

Most studies on semantic segmentation use programming algorithms beyond the software available to BIM operators. This work advances upon the applicability of the CANUPO software, which is a plug-in to C2C, well known within the scientific community. This algorithm was tested to verify that semantic segmentation can provide a representative sample point set to mesh and subsequently build parametric BIM objects. To do this, point cloud data from elements analysed within the façade of the 16th-century Casa de Pilatos Palace in Seville, Spain, were considered. Brodu and Lague's natural surface classification algorithm cannot detect the presence of changing materials on the same surface but works by the degree of geometric heterogeneity, where a single scale can rarely classify a scene [7]. To test its applicability to CH, the aforementioned façade was taken, which presents several complex geometries of different architectural styles, thus being a suitable example for experimentation. Three testbeds were carried out; first, the architectural elements comprising the entire façade; second, on the main gate; and third, on a small retable located on the left side of the façade canvas. Results on the first testbed show that the classification is less dispersed (test A) by considering low values (Table 2). In test D, the accuracy increases, as does the number of unclassified points. The accuracy determines the number of points the algorithm can detect. This could indicate that points may not be properly classified. To achieve an adequate classification of the points, it was considered that the representativeness should be at least 75 % of the global set and sufficiently sparse for Mesh-to-BIM. The classification must be based on a previous decimation of the point subsets (section 4 of this paper). In the second testbed, test F shows a higher accuracy and marble and wood are above the unclassified ones. The higher the accuracy, the more significant the points of the wooden door are. In the last testbed (retable), the classification did not distinguish between architectural elements. Here, the automatic segmentation process presented serious difficulties for comprehensive modelling as in Figure 18. Therefore, the exact control of the geometry of the wooden entrance door is questionable. In view of the results, the CANUPO classification algorithm is more successful on large complex façades than on minor details such as the small marble retable. In this case, the algorithm fails to classify the elements of the cross concerning the planes and elements of the cornice. The tested scale yields a better classification when the base exceeds 10 metres in length.

Another interesting parameter is the time the algorithm takes to classify the selected point sets. This variable is of interest to the BIM operator, as it influences the operational performance of the process. Generally speaking, the processing time in tests A, B and C for both classification and training was a few minutes. Meanwhile, in test D, where the maximum training distance was taken, the time was approximately 12 minutes and 6 minutes for classification. In this case, the percentages of classified points were even lower than 70 %. For the second testbed, the results could be improved, since the processing time was 14 minutes for 61.91% of classified points. In the third testbed, the processing time was 5 minutes for 95.75% of classified points, although no positive classification results were obtained. Therefore, a multiscale point cloud analysis was introduced to semantically segment architectural elements through an open-source algorithm accessible to all researchers, academics and professionals in the Architecture, Engineering and Construction (AEC) industry.

The creation of cross-sections of the wooden door parametric model revealed heterogeneity of the points and the morphology achieved with respect to the TLS data and the semantic segmentation model. The results determined the absence of points in important parts in the point set post-processing for Mesh-to-BIM. The percentage of gaps is due to the partial segmentation by the classification algorithm, thus losing part of the important elements for meshing. Part of the classification point sets yielded non-representative data. Figure 25 shows the results of two tests of the meshing of the wooden door using C2C and the CANUPO algorithm.

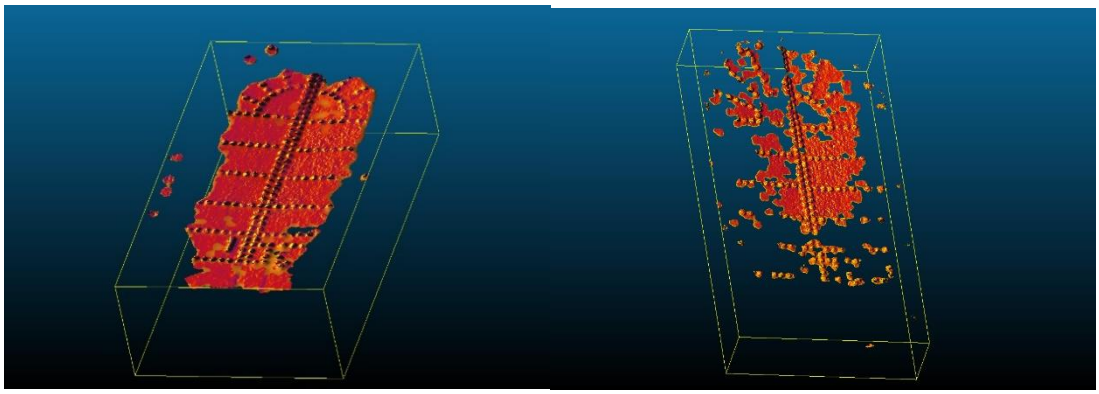

Figure 25. The meshing of the wooden door in C2C. (a) Test E. (b) Test F.

The validation of the point set decimation for Mesh-to-BIM determines that a density of at least 600 points per square metre in the segmentation is necessary to obtain a representative sample of the mesh for BIM parameterisation. According to Pu and Vosselman [30], over-segmentation is preferable to under-segmentation when large elements coexist. In this paper (section 4.2), a minimum spacing of 6 centimetres is recommended as the optimal value for a subset of segmented points.

Conclusions

In this work, the applicability of Brodu and Lague's algorithm [7] was explored in architectural elements of heritage sites. Based on the acquisition of TLS data from a façade of the Casa de Pilatos Palace, an experimental process was developed through three testbeds. A semantic segmentation method was followed based on open-source software applications such as C2C that are easy to use by operators, academics and BIM researchers, without the need for programming. Therefore, the aim was to recognise common morphological features in heritage buildings, so that complex geometries could be identified.

As explained above, the use of these algorithms is sometimes not within the reach of the usual BIM operators. Firstly, the programmes used generally derive from mathematical work, which requires a process and knowledge in computational mathematics and visual geometry. Secondly, not all point cloud data captured by acquisition techniques such as TLS or SfM are valid. Most segmentation algorithms work with structured or LiDAR files only.

Brodu and Lague developed the system on natural scenes of a subset to recognise rocks, vegetation, water, and gravel in a riverbed. However, this work aimed to experiment with the geometric fidelity that semantic segmentation can achieve for classifying architectural elements under CANUPO plug-in training. Given that these tests have not been applied before,

632 the methodology adopted is original. Also, the validation analysis of the Mesh-to-BIM process
633 has not been presented before. In order to select the most suitable process to obtain data for
634 HBIM parameterisation, the results of the algorithm were compared with the manual
635 segmentation and the selected point set was evaluated. Examining these subsets is essential to
636 verify their suitability for accurate 3D geometric reconstruction. This paper also discusses an
637 optimisation framework to analyse other segmentation software to produce parametric BIM
638 objects.

639 In the experimental tests, the algorithm was found to be a classifier of morphological surfaces
640 since when there is no variation in morphology, the algorithm cannot classify the data, as
641 occurred in the retablo test. Furthermore, it is worth mentioning that, as shown in the results
642 of tests E and F from the 3D mesh reconstruction, the absence of point sets does not imply a
643 complete surface. As a result, a complete segmentation would yield better results for
644 transformation into parametric objects. It was also demonstrated that the classification
645 algorithm, previously implemented on surfaces more complex than those of traditional
646 architectural shapes, entails a reduction in accuracy for small scales.

647 On the other hand, optimal values of the segmentation parameters were sought so that
648 representative data for Mesh-to-BIM could be obtained with the smallest number of points.
649 Testbeds were carried out from 100 to 600 points per square metre to determine the required
650 segmentation point density for BIM. It was determined that the point spacing should be at
651 least 6 cm and uniform over the entire surface of the objects. Therefore, the results of the
652 automatic segmentation by the CANUPO algorithm are not optimal for parameterising
653 architectural elements in a BIM environment. The reason lies in the lack of essential points in
654 certain areas and the presence of excessive gaps caused by the non-classification of points.

655 One of the main issues of this classifier is that, in the testbed of the wooden door, the
656 algorithm determined points that did not belong to that subset (false positives) and
657 accordingly classified them outside the surface. This is when the BIM operator has to intervene
658 to analyse and interpret the data. Nevertheless, the algorithm yielded positive data of scale
659 proportionality. Regarding the third testbed, the results showed no classification subsets. The
660 aim was to segment the cross, but the uniformity of the points indicated that the algorithm
661 was unable to perform such segmentation.

662 Future work will not only adapt this algorithm to improve its applicability efficiency but also
663 conduct further research based on it to meet the requirements of integrating point sets into
664 BIM. These requirements are the uniformity in the point dispersion (which is related to the
665 resolution of the set) and that the decimation exceeds 85 % of the total number of source
666 points. Besides, geometric and colourimetric segmentation can be combined to classify TLS
667 and SfM point clouds, which are characterised by geometric and colourimetric features. The
668 algorithm was developed to classify terrain, vegetation, or gravel, achieving a classification
669 accuracy of 98% when separating vegetation from the soil. However, it was not possible to
670 achieve the same performance for less complex architectural features without excessive
671 roughness.

672 **References**

673 [1] C. Bolognesi, V. Caffi, Extration of Primitives and Objects from Hshapes, ISPRS Ann.
674 Photogramm. Remote Sens. Spat. Inf. Sci. XLII-2/W9 (2019) 151–156.
675 https://doi.org/10.5194/isprs-archives-XLII-2-W9-151-2019.

[2] S. Bruno, M. De Fino, F. Fatiguso, Historic Building Information Modelling: performance assessment for diagnosis-aided information modelling and management, Autom. Constr. 86 (2018) 256–276. https://doi.org/10.1016/j.autcon.2017.11.009.

[3] J.E. Nieto-Julián, L. Lara, J. Moyano, Implementation of a TeamWork-HBIM for the Management and Sustainability of Architectural Heritage, Sustainability. 13 (2021) 2161. https://doi.org/10.3390/su13042161.

[4] M. Murphy, E. McGovern, S. Pavia, Historic Building Information Modelling - Adding intelligence to laser and image based surveys of European classical architecture, ISPRS J. Photogramm. Remote Sens. 76 (2013) 89–102. https://doi.org/10.1016/j.isprsjprs.2012.11.006.

[5] R. Pierdicca, M. Paolanti, F. Matrone, M. Martini, C. Morbidoni, E.S. Malinverni, E. Frontoni, A.M. Lingua, Point Cloud Semantic Segmentation Using a Deep Learning Framework for Cultural Heritage, Remote Sens. 12 (2020) 1005. https://doi.org/10.3390/rs12061005.

[6] G. Patrucco, F. Chiabrando, A. Dameri, L.T. Losè, Geomatic contribution for the restoration project of the valentino castle green room. from data acquisition to integrated documentation, Int. Arch. Photogramm. Remote Sens. Spat. Inf. Sci. XLIII-B2 (2020) 885–892. https://doi.org/10.5194/isprs-archives-xliii-b2-2020-885-2020.

[7] N. Brodu, D. Lague, 3D terrestrial lidar data classification of complex natural scenes using a multi-scale dimensionality criterion: Applications in geomorphology, ISPRS J. Photogramm. Remote Sens. 68 (2012) 121–134. https://doi.org/10.1016/j.isprsjprs.2012.01.006.

[8] Daniel Girardeau-Montaut, D. CloudCompare: 3D point cloud and mesh processing software. Open Source Project 2016., (n.d.). https://www.danielgm.net/index.php (accessed May 9, 2019).

[9] MoBiVAP Research Croup, Reconstrucción 3D, in: Reconstrucción 3D, 2013: p. 15. http://lfa.mobivap.uva.es/~cevic/wp-content/uploads/2015/01/preface02.pdf.

[10] S.F. El-Hakim, J.A. Beraldin, M. Picard, G. Godin, Detailed 3D reconstruction of large-scale heritage sites with integrated techniques, IEEE Comput. Graph. Appl. 24 (2004) 21–29. https://doi.org/10.1109/MCG.2004.1318815.

[11] L. Gomes, O. Regina Pereira Bellon, L. Silva, 3D reconstruction methods for digital preservation of cultural heritage: A survey, Pattern Recognit. Lett. 50 (2014) 3–14. https://doi.org/10.1016/j.patrec.2014.03.023.

[12] S. Ochmann, R. Vock, R. Klein, Automatic reconstruction of fully volumetric 3D building models from oriented point clouds, ISPRS J. Photogramm. Remote Sens. 151 (2019) 251–262. https://doi.org/10.1016/j.isprsjprs.2019.03.017.

[13] M. Gaiani, B. Benedetti, F.I. Apollonio, Teorie per rappresentare e comunicare i siti archeologici attraverso modelli critici, SCIRES-IT Sci. Res. Inf. Technol. 1 (2011) 33–70. https://doi.org/10.2423/i22394303v1n2p33.

[14] L. De Luca, P. Veron, M. Florenzano, Reverse engineering of architectural buildings based on a hybrid modeling approach, Comput. Graph. 30 (2006) 160–176. https://doi.org/10.1016/j.cag.2006.01.020.

[15] A. Fryskowska, J. Stachelek, A no-reference method of geometric content quality analysis of 3D models generated from laser scanning point clouds for hBIM, J. Cult.

720 Herit. 34 (2018) 95–108. https://doi.org/10.1016/J.CULHER.2018.04.003.

721 [16] A.A. Fernández, E. Soria, L. Agustín, J. Alberto, A. Adrián, B. Ereño, E. Salvador, I. Jordán,
722 E. Nieto, J.J. Moyano, J. Antonio Herráez, Y. Espinosa, J. Leache, A. Rafael, M.
723 Talaverano, A. Mahillo, J. González, A. José, I. Murillo, F. Carlos, R. María, I. Sardón, D.
724 De Autor, BIM aplicado al Patrimonio Cultural Coordinador del proyecto Coordinadores
725 de los grupos de trabajo, (2018).
726 https://www.researchgate.net/profile/Juan_Nieto10/publication/330183791_BIM_apli
727 cado_al_Patrimonio_Cultural_Documento_14_Guia_de_usuarios_BIM_Building_SMAR
728 T_Spain_Chapter/links/5c328768299bf12be3b3ed0d/BIM-aplicado-al-Patrimonio-
729 Cultural-Documento-14-Guia (accessed January 7, 2020).

730 [17] V. Bagnolo, R. Argiolas, A. Cuccu, HBIM for archaeological sites: from SFM based survey
731 to algorithmic modeling, Int. Arch. Photogramm, Remote Sens. Spat. Inf. Sci. XLII–2
732 (2019) 57–63. https://doi.org/10.5194/isprs-archives-XLII-2-W9-57-2019.

733 [18] H.M. Yilmaz, M. Yakar, S.A. Gulec, O.N. Dulgerler, Importance of digital close-range
734 photogrammetry in documentation of cultural heritage, J. Cult. Herit. 8 (2007) 428–433.
735 https://doi.org/10.1016/j.culher.2007.07.004.

736 [19] F. Chiabrando, M. Lo Turco, C. Santagati, Digital invasions: From point clouds to
737 historical building object modeling (h-BOM) of a unesco WHL site, Int. Arch.
738 Photogramm. Remote Sens. Spat. Inf. Sci. - ISPRS Arch. 42 (2017) 171–178.
739 https://doi.org/10.5194/isprs-archives-XLII-2-W3-171-2017.

740 [20] L. Klein, N. Li, B. Becerik-Gerber, Imaged-based verification of as-built documentation of
741 operational buildings, Autom. Constr. 21 (2012) 161–171.
742 https://doi.org/10.1016/j.autcon.2011.05.023.

743 [21] J. Moyano, J.E. Nieto-Julián, D. Bienvenido-Huertas, D. Marín-García, Validation of
744 Close-Range Photogrammetry for Architectural and Archaeological Heritage: Analysis of
745 Point Density and 3d Mesh Geometry, Remote Sens. 12 (2020) 3571.
746 https://doi.org/10.3390/rs12213571.

747 [22] P. Tang, D. Huber, B. Akinci, R. Lipman, A. Lytle, Automatic reconstruction of as-built
748 building information models from laser-scanned point clouds: A review of related
749 techniques, Autom. Constr. 19 (2010) 829–843.
750 https://doi.org/10.1016/j.autcon.2010.06.007.

751 [23] J.A.H. Tortosa, D.T. Fuentes, M.L. Cereceda, Y.S. Berrio, The façade of the church of
752 nuestra señora de la asunción in biar (Spain): From point cloud to HBIM, WIT Trans.
753 Built Environ. 169 (2017) 69–77. https://doi.org/10.2495/BIM170071.

754 [24] A. Baik, From point cloud to Jeddah Heritage BIM Nasif Historical House – case study,
755 Digit. Appl. Archaeol. Cult. Herit. 4 (2017) 1–18.
756 https://doi.org/10.1016/J.DAACH.2017.02.001.

757 [25] J. Jung, S. Hong, S. Jeong, S. Kim, H. Cho, S. Hong, J. Heo, Productive modeling for
758 development of as-built BIM of existing indoor structures, Autom. Constr. 42 (2014) 68–
759 77. https://doi.org/10.1016/j.autcon.2014.02.021.

760 [26] X. Yang, P. Grussenmeyer, M. Koehl, H. Macher, A. Murtiyoso, T. Landes, Review of built
761 heritage modelling: Integration of HBIM and other information techniques, J. Cult.
762 Herit. 46 (2020) 350–360. https://doi.org/10.1016/j.culher.2020.05.008.

763 [27] S. Spina, K. Debattista, K. Bugeja, A. Chalmers, Point Cloud Segmentation for Cultural

764 Heritage Sites, VAST Int. Symp. Virtual Reality, Archaeol. Intell. Cult. Herit. (2011) 41–
765 48. https://doi.org/10.2312/VAST/VAST11/041-048.

766 [28] H. Macher, T. Landes, P. Grussenmeyer, From point clouds to building information
767 models: 3D semi-automatic reconstruction of indoors of existing buildings, Appl. Sci. 7
768 (2017) 1–30. https://doi.org/10.3390/app7101030.

769 [29] E. Grilli, F. Menna, F. Remondino, A review of point clouds segmentation and
770 classification algorithms., Int. Arch. Photogramm. Remote Sens. Spat. Inf. Sci. XLII-2/W3
771 (2017) 340–344. https://doi.org/10.5194/isprs-archives-XLII-2-W3-339-2017.

772 [30] S. Pu, G. Vosselman, Knowledge based reconstruction of building models from
773 terrestrial laser scanning data, ISPRS J. Photogramm. Remote Sens. 64 (2009) 575–584.
774 https://doi.org/10.1016/j.isprsjprs.2009.04.001.

775 [31] F. Boochs, A. Marbs, H. Hmida, H. Truong, A. Karmachaiya, C. Cruz, A. Habed, C. Nicolle,
776 Y. Voisin, Integration of knowledge to support automatic object reconstruction from
777 images and 3D data, in: Eighth Int. Multi-Conference Syst. Signals Devices, Institute of
778 Electrical and Electronics Engineers (IEEE), 2011: pp. 1–13.
779 https://doi.org/10.1109/ssd.2011.5993558.

780 [32] X. Lu, A.K. Jain, D. Colbry, Matching 2.5D face scans to 3D models, IEEE Trans. Pattern
781 Anal. Mach. Intell. 28 (2006) 31–42. https://doi.org/10.1109/TPAMI.2006.15.

782 [33] S. Ochmann, R. Vock, R. Wessel, R. Klein, Automatic reconstruction of parametric
783 building models from indoor point clouds, Comput. Graph. 54 (2016) 94–103.
784 https://doi.org/10.1016/J.CAG.2015.07.008.

785 [34] S. Hong, J. Jung, S. Kim, H. Cho, J. Lee, J. Heo, Semi-automated approach to indoor
786 mapping for 3D as-built building information modeling, Comput. Environ. Urban Syst.
787 51 (2015) 34–46. https://doi.org/10.1016/J.COMPENVURBSYS.2015.01.005.

788 [35] C. Thomson, J. Boehm, Automatic geometry generation from point clouds for BIM,
789 Remote Sens. 7 (2015) 11753–11775. https://doi.org/10.3390/rs70911753.

790 [36] T. Rabbani, F.A. Van Den Heuvel, G. Vosselman, Segmentation of point clouds using
791 smoothness constraint, Int. Arch. Photogramm. Remote Sens. Spat. Inf. Sci. - ISPRS
792 Arch. 36 (2006) 248–253.

793 [37] M.A. Wani, H.R. Arabnia, Parallel edge-region-based segmentation algorithm targeted
794 at reconfigurable MultiRing network, J. Supercomput. 25 (2003) 43–62.
795 https://doi.org/10.1023/A:1022804606389.

796 [38] T. Rabbani, F.A. Van Den Heuvel, G. Vosselman, Segmentation of point clouds using
797 smoothness constraint, Int. Arch. Photogramm. Remote Sens. Spat. Inf. Sci. - ISPRS
798 Arch. 36 (2006) 248–253.

799 [39] M.A. Fischler, R.C. Bolles, RANSAC1981.pdf, Graph. Image Process. 24 (1981) 381–395.
800 https://doi.org/10.1145/358669.358692.

801 [40] M. Andriasyan, J. Moyano, J.E. Nieto-Julián, D. Antón, From Point Cloud Data to Building
802 Information Modelling: An Automatic Parametric Workflow for Heritage, Remote Sens.
803 2020, Vol. 12, Page 1094. 12 (2020) 1094. https://doi.org/10.3390/RS12071094.

804 [41] D. Antón, B. Medjdoub, R. Shrahily, J. Moyano, Accuracy evaluation of the semi-
805 automatic 3D modeling for historical building information models, Int. J. Archit. Herit.
806 12 (2018) 790–805. https://doi.org/10.1080/15583058.2017.1415391.

[42] L. Barazzetti, Parametric as-built model generation of complex shapes from point clouds, Adv. Eng. Informatics. 30 (2016) 298–311. https://doi.org/10.1016/j.aei.2016.03.005.

[43] C. Dore, M. Murphy, Semi-Automatic Generation of As- Built Bim Façade Geometry From Laser and Image Data, 19 (2014) 20–46.

[44] M. Zheliazkova, R. Naboni, I. Paoletti, A parametric-assisted method for 3D generation of as-built BIM models for the built heritage, in: Struct. Stud. Repairs Maint. Herit. Archit. XIV, WIT Press, 2015: pp. 693–704. https://doi.org/10.2495/str150581.

[45] B. Rivera, P. Merchán, S. Salamanca, E. Pérez, M.D. Moreno, M.J. Merchán, Creación de bibliotecas de objetos paramétricos para su integración en modelo HBIM, in: Actas Las XXXIX Jornadas Automática, Badajoz, 5-7 Septiembre 2018, 2018: pp. 1069–1076.

[46] K. Aitelkadi, D. Tahiri, E. Simonetto, I. Sebari, L. Polidori, Segmentation of heritage building by means of geometric and radiometric components from terrestrial laser scanning, ISPRS Ann. Photogramm. Remote Sens. Spat. Inf. Sci. 2 (2013) 1–6. https://doi.org/10.5194/isprsannals-II-5-W1-1-2013.

[47] S. Gonizzi Barsanti, G. Guidi, L. De Luca, Segmentation of 3D models for cultural heritage structural analysis - some critical some issues, ISPRS Ann. Photogramm. Remote Sens. Spat. Inf. Sci. 4 (2017) 115–122. https://doi.org/10.5194/isprs-annals-IV-2-W2-115-2017.

[48] P.C. Library, Point Cloud Library | The Point Cloud Library (PCL) is a standalone, large scale, open project for 2D/3D image and point cloud processing., (2020). https://pointclouds.org/ (accessed January 7, 2021).

[49] H. Ding, X. Jiang, B. Shuai, A.Q. Liu, G. Wang, Semantic Segmentation with Context Encoding and Multi-Path Decoding, IEEE Trans. Image Process. 29 (2020) 3520–3533. https://doi.org/10.1109/TIP.2019.2962685.

[50] G.I. Penagos-Londoño, C. Rodriguez-Sanchez, F. Ruiz-Moreno, E. Torres, A machine learning approach to segmentation of tourists based on perceived destination sustainability and trustworthiness, J. Destin. Mark. Manag. 19 (2021) 100532. https://doi.org/10.1016/j.jdmm.2020.100532.

[51] J. Llamas, P. M. Lerones, R. Medina, E. Zalama, J. Gómez-García-Bermejo, Classification of Architectural Heritage Images Using Deep Learning Techniques, Appl. Sci. 7 (2017) 992. https://doi.org/10.3390/app7100992.

[52] E.-K. Stathopoulou, F. Remondino, Semantic photogrammetry -Boosting image-based 3D reconstruction with semantic labeling., ISPRS - Int. Arch. Photogramm. Remote Sens. Spat. Inf. Sci. XLII-2/W9 (2019) 685–690. https://doi.org/10.5194/isprs-archives-XLII-2-W9-685-2019.

[53] Z. Wu, S. Song, A. Khosla, Y. Fisher, L. Zhang, X. Tang, J. Xiao, 3D ShapeNets: A Deep Representation for Volumetric Shapes, 2015. http://3dshapenets.cs.princeton.edu (accessed February 10, 2021).

[54] C.R. Qi, H. Su, K. Mo, L.J. Guibas, PointNet: Deep learning on point sets for 3D classification and segmentation, in: Proc. - 30th IEEE Conf. Comput. Vis. Pattern Recognition, CVPR 2017, Institute of Electrical and Electronics Engineers Inc., 2017: pp. 77–85. https://doi.org/10.1109/CVPR.2017.16.

[55] N. Oses, F. Dornaika, A. Moujahid, Image-Based Delineation and Classification of Built

Heritage Masonry, Remote Sens. 6 (2014) 1863–1889. https://doi.org/10.3390/rs6031863.

[56] G. Bitelli, G. Castellazzi, A.M. D'altri, S. De Miranda, A. Lambertini, I. Selvaggi, Automated voxel model from point clouds for structural analysis of cultural heritage, in: Int. Arch. Photogramm. Remote Sens. Spat. Inf. Sci. - ISPRS Arch., International Society for Photogrammetry and Remote Sensing, 2016: pp. 191–197. https://doi.org/10.5194/isprsarchives-XLI-B5-191-2016.

[57] T. Hinks, H. Carr, L. Truong-Hong, D.F. Laefer, Point Cloud Data Conversion into Solid Models via Point-Based Voxelization, J. Surv. Eng. 139 (2013) 72–83. https://doi.org/10.1061/(asce)su.1943-5428.0000097.

[58] M. Rouse, ¿Qué es vóxel? - Definición de WhatIs.com, (2015). https://whatis.techtarget.com/definition/voxel (accessed February 10, 2021).

[59] C. Wang, Y.K. Cho, C. Kim, Automatic BIM component extraction from point clouds of existing buildings for sustainability applications, Autom. Constr. 56 (2015) 1–13. https://doi.org/10.1016/j.autcon.2015.04.001.

[60] M. Ye, S. Xu, T. Cao, HVNet: Hybrid Voxel Network for LiDAR Based 3D Object Detection, in: Proc. IEEE Comput. Soc. Conf. Comput. Vis. Pattern Recognit., IEEE Computer Society, 2020: pp. 1628–1637. https://doi.org/10.1109/CVPR42600.2020.00170.

[61] Q. Lu, S. Lee, Image-Based Technologies for Constructing As-Is Building Information Models for Existing Buildings, J. Comput. Civ. Eng. 31 (2017) 04017005. https://doi.org/10.1061/(asce)cp.1943-5487.0000652.

[62] J. Moyano, J.E. Nieto-Julián, D. Antón, E. Cabrera, D. Bienvenido-Huertas, N. Sánchez, Suitability Study of Structure-from-Motion for the Digitisation of Architectural (Heritage) Spaces to Apply Divergent Photograph Collection, Symmetry (Basel). 12 (2020) 1981. https://doi.org/10.3390/sym12121981.

[63] Ľ. Kovanič, P. Blistan, R. Urban, M. Štroner, K. Pukanská, K. Bartoš, J. Palková, Analytical determination of geometric parameters of the rotary kiln by novel approach of tls point cloud segmentation, Appl. Sci. 10 (2020) 1–27. https://doi.org/10.3390/app10217652.

[64] Z. Li, L. Zhang, P.T. Mathiopoulos, F. Liu, L. Zhang, S. Li, H. Liu, A hierarchical methodology for urban facade parsing from TLS point clouds, ISPRS J. Photogramm. Remote Sens. 123 (2017) 75–93. https://doi.org/10.1016/j.isprsjprs.2016.11.008.

[65] C. Paris, D. Kelbe, J. Van Aardt, L. Bruzzone, A Novel Automatic Method for the Fusion of ALS and TLS LiDAR Data for Robust Assessment of Tree Crown Structure, IEEE Trans. Geosci. Remote Sens. 55 (2017) 3679–3693. https://doi.org/10.1109/TGRS.2017.2675963.

[66] A. Burt, M. Disney, K. Calders, Extracting individual trees from lidar point clouds using *treeseg*, Methods Ecol. Evol. 10 (2018) 2041–210X.13121. https://doi.org/10.1111/2041-210X.13121.

[67] F. Bosché, M. Ahmed, Y. Turkan, C.T. Haas, R. Haas, The value of integrating Scan-to-BIM and Scan-vs-BIM techniques for construction monitoring using laser scanning and BIM: The case of cylindrical MEP components, Autom. Constr. 49 (2015) 201–213. https://doi.org/10.1016/j.autcon.2014.05.014.

[68] Q. Wang, J. Guo, M.-K. Kim, An Application Oriented Scan-to-BIM Framework, Remote Sens. 11 (2019) 365. https://doi.org/10.3390/rs11030365.

[69] J. Moyano, C.P. Odriozola, J.E. Nieto-Julián, J.M. Vargas, J.A. Barrera, J. León, Bringing BIM to archaeological heritage: Interdisciplinary method/strategy and accuracy applied to a megalithic monument of the Copper Age, J. Cult. Herit. (2020). https://doi.org/10.1016/j.culher.2020.03.010.

[70] L. Ma, R. Favier, L. Do, E. Bondarev, P.H.N. De With, Plane segmentation and decimation of point clouds for 3D environment reconstruction, in: 2013 IEEE 10th Consum. Commun. Netw. Conf. CCNC 2013, IEEE, 2013: pp. 43–49. https://doi.org/10.1109/CCNC.2013.6488423.

[71] X. Yang, Y.-C. Lu, A. Murtiyoso, M. Koehl, P. Grussenmeyer, HBIM Modeling from the Surface Mesh and Its Extended Capability of Knowledge Representation, Isprs Int. J. Geo-Inf. 8 (2019) 301. https://doi.org/10.3390/ijgi8070301.

[72] M. Kazhdan, H. Hoppe, Screened poisson surface reconstruction, ACM Trans. Graph. 32 (2013) 1–13. https://doi.org/10.1145/2487228.2487237.